Обзор ArXiv/astro-ph, 9-14 июня 2022

От Сильченко О.К.

ArXiv: 2206.05217

Bulge formation inside quiescent lopsided stellar disks: connecting accretion, star formation and morphological transformation in a z ∼ 3 galaxy group

Boris S. Kalita[1], Emanuele Daddi[1], Frederic Bournaud[1], R. Michael Rich[2], Francesco Valentino[3,4], Carlos Gómez-Guijarro[1], Sandrine Codis[1], Ivan Delvecchio[5], David Elbaz[1], Veronica Strazzullo[6,7,8], Victor de Sousa Magalhaes[8], Jérôme Pety[9], and Qinghua Tan[10,1]

[1] CEA, Irfu, DAp, AIM, Universitè Paris-Saclay, Universitè de Paris, CNRS, F-91191 Gif-sur-Yvette, France
[2] Department of Physics & Astronomy, University of California Los Angeles, 430 Portola Plaza, Los Angeles, CA 90095, USA
[3] Cosmic Dawn Center (DAWN)
[4] Niels Bohr Institute, University of Copenhagen, Jagtvej 128, DK-2200, Copenhagen N, Denmark
[5] INAF — Osservatorio Astronomico di Brera, via Brera 28, I-20121, Milano, Italy
[6] University of Trieste, Piazzale Europa, 1, 34127 Trieste TS, Italy
[7] INAF — Osservatorio Astronomico di Brera, via Brera 28, I-20121, Milano, Italy
[8] INAF — Osservatorio Astronomico di Trieste, via Tiepolo 11, I-34131, Trieste, Italy
[9] Institut de Radioastronomie Millimétrique, 300 Rue de la Piscine, F-38406 Saint Martin d'Hères, France
[10] Purple Mountain Observatory & Key Laboratory for Radio Astronomy, Chinese Academy of Sciences, 10 Yuanhua Road, Nanjing 210023, People's Republic of China

Accepted for publication in A&A

ABSTRACT

We present well-resolved near-IR and sub-mm analysis of the three highly star-forming massive ($> 10^{11}\,M_\odot$) galaxies within the core of the RO-1001 galaxy group at z = 2.91. Each of them displays kpc-scale compact star-bursting cores with properties consistent with forming galaxy bulges, embedded at the center of extended, massive stellar disks. Surprisingly, the stellar disks are unambiguously both quiescent, and severely lopsided. Therefore, 'outside-in' quenching is ongoing in the three group galaxies. We propose an overall scenario in which the strong mass lopsidedness in the disks (ranging from factors of 1.6 to >3), likely generated under the effects of accreted gas and clumps, is responsible for their star-formation suppression, while funnelling gas into the nuclei and thus creating the central starbursts. The lopsided side of the disks marks the location of accretion streams impact, with additional matter components (dust and stars) detected in their close proximity directly tracing the inflow direction. The interaction with the accreted clumps, which can be regarded as minor-mergers, leads the major axes of the three galaxies to be closely aligned with the outer Lyman-α-emitting feeding filaments. These results provide the first observational evidence of the impact of cold accretion streams on the formation and evolution of the galaxies they feed. In the current phase, this is taking the form of the rapid buildup of bulges under the effects of accretion, while still preserving massive quiescent and lopsided stellar disks at least until encountering a violent major-merger.

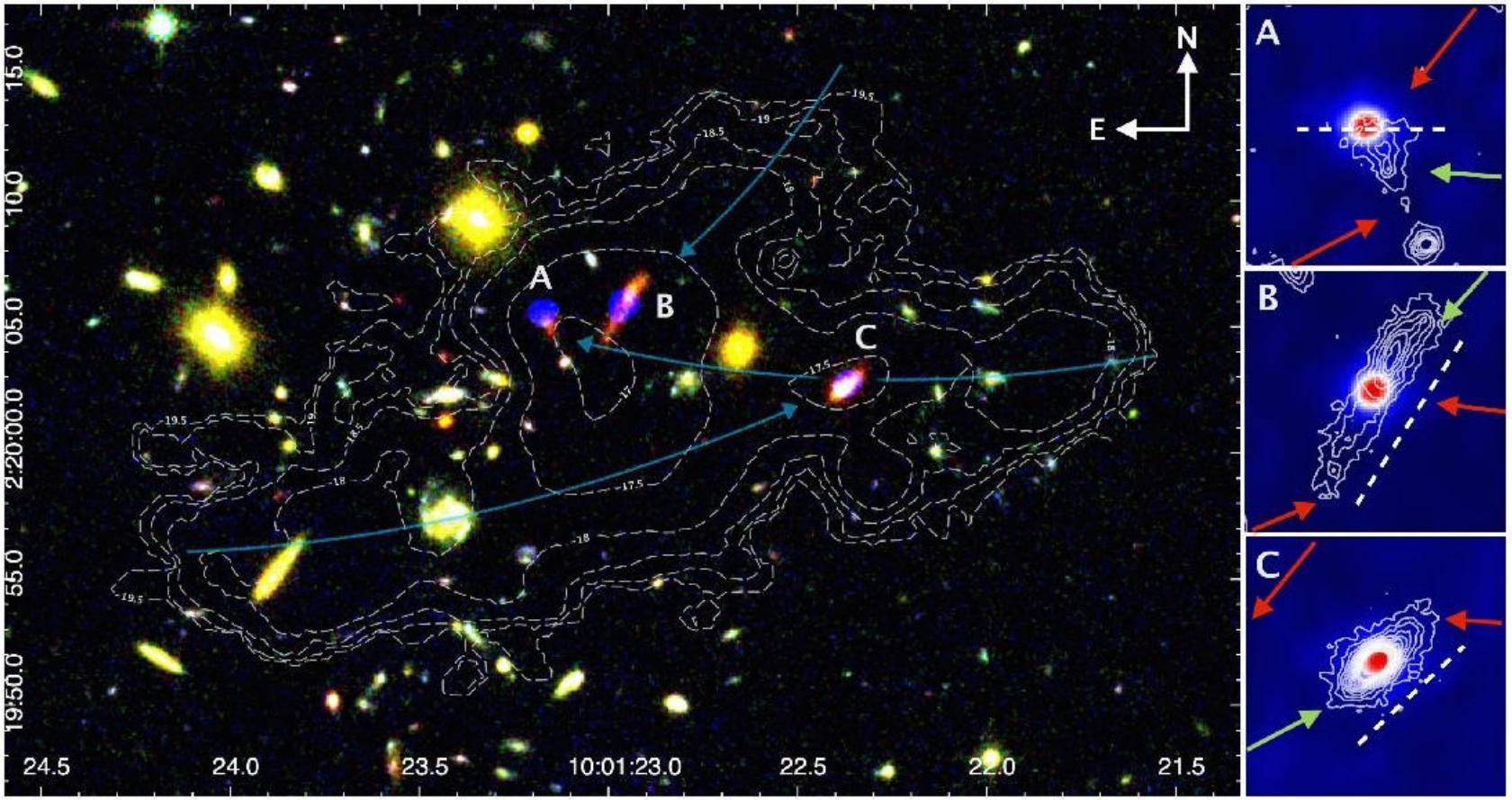

Fig. 1. Location of the massive star-forming galaxies in the network of Lyman-α filaments. (Left) Color image composite of RO-1001, using observations in F160W, F125W and F606W. The ALMA data has been co-added to that in F606W since both trace star-formation, differing based on dust obscuration. The scaling of the ALMA data was done based on its flux to SFR ratio in comparison to the same for that in F606W. The white dashed contours trace the Lyman-α halo whereas the cyan arrows show the tentative directions of the three gas-accretion filaments converging onto the center of the group potential well (the correspondence to the galaxies is discussed in detail in Sec. 5.2). (Right) Zoom on the three star-forming galaxies (A, B and C) as seen in ALMA sub-millimeter dust-emission while the white contours trace the F160W flux tracing stellar light. The contours begin at 4σ with increments of 4σ. The arrows indicate the direction of the streams, which are shown in green if they are aligned with the major axis of the galactic disks (in dashed white lines), as discussed in Sec. 5.2. Those which are not, are in red. In case of Galaxy-A, we rather show the major axis of the ALMA contour with the white dashed line.

Свойства трех галактик

Table 1. Properties of the star-forming massive galaxies in RO-1001

ID		A	B	C
RA		10:01:23.174	10:01:22.964	10:01:22.369
DEC		02:20:05.57	02:20:05.87	02:20:02.63
$z_{\rm spec}$		2.9214	2.9156	2.9064
$\log M_\star$ (1)	$M_\odot$	$11.50^{+0.15}_{-0.19}$	$11.20^{+0.07}_{-0.14}$	$11.26^{+0.14}_{-0.10}$
$S_\nu(870\,\mu{\rm m})$	mJy	4.44 ± 0.05	8.69 ± 0.03	4.04 ± 0.11
SFR_{core} (2)	$M_\odot\ yr^{-1}$	345 ± 55	674 ± 106	313 ± 50
SFR_{disk_ALMA} (2)	$M_\odot\ yr^{-1}$	$< 60^{**}$	$< 19^{**}$	$< 43^{**}$
SFR_{disk_SED} (1)	$M_\odot\ yr^{-1}$	66^{+446}_{-49} (3)	42^{+51}_{-37}	94^{+66}_{-94}
t_{50} (1)	Gyr	$1.7^{+0.3}_{-0.7}$	$0.5^{+0.7}_{-0.2}$	$0.2^{+1.3}_{-0.1}$
r_{e_disk}	kpc	3 ± 1	9 ± 2	4 ± 1
r_{disk}/r_{core}		4 ± 1	9 ± 2	5 ± 1
$\log M_{mol}$	$M_\odot$	9.8	10.7	10.6
$FWZV_{CO[3-2]}$ (4)	km s^{-1}	381	1114	1098
$\log M_{dyn,tot}$ (5)	$M_\odot$	10.4	11.1	11.2
A_v		$1.8^{2.1}_{1.3}$	$1.0^{1.2}_{0.4}$	$1.6^{1.8}_{0.4}$

Notes: (1) Estimated from the composite-τ model fitting to optical and near-IR photometry and therefore primarily associated with the disks (2) Derived from the 870μm flux of individual galaxies assuming the same SED shape as for their coaddition (Daddi et al. 2021). (3) This high upper-limit from the composite-τ model is in agreement with a constant star formation model being within 90% confidence interval (4) Full Width at Zero Velocity as previously reported (Daddi et al. 2021). (5) Dynamical mass primarily associated with the core, rather than the whole galaxy as described in the main text. ** 3σ upper-limits.

Асимметричные диски

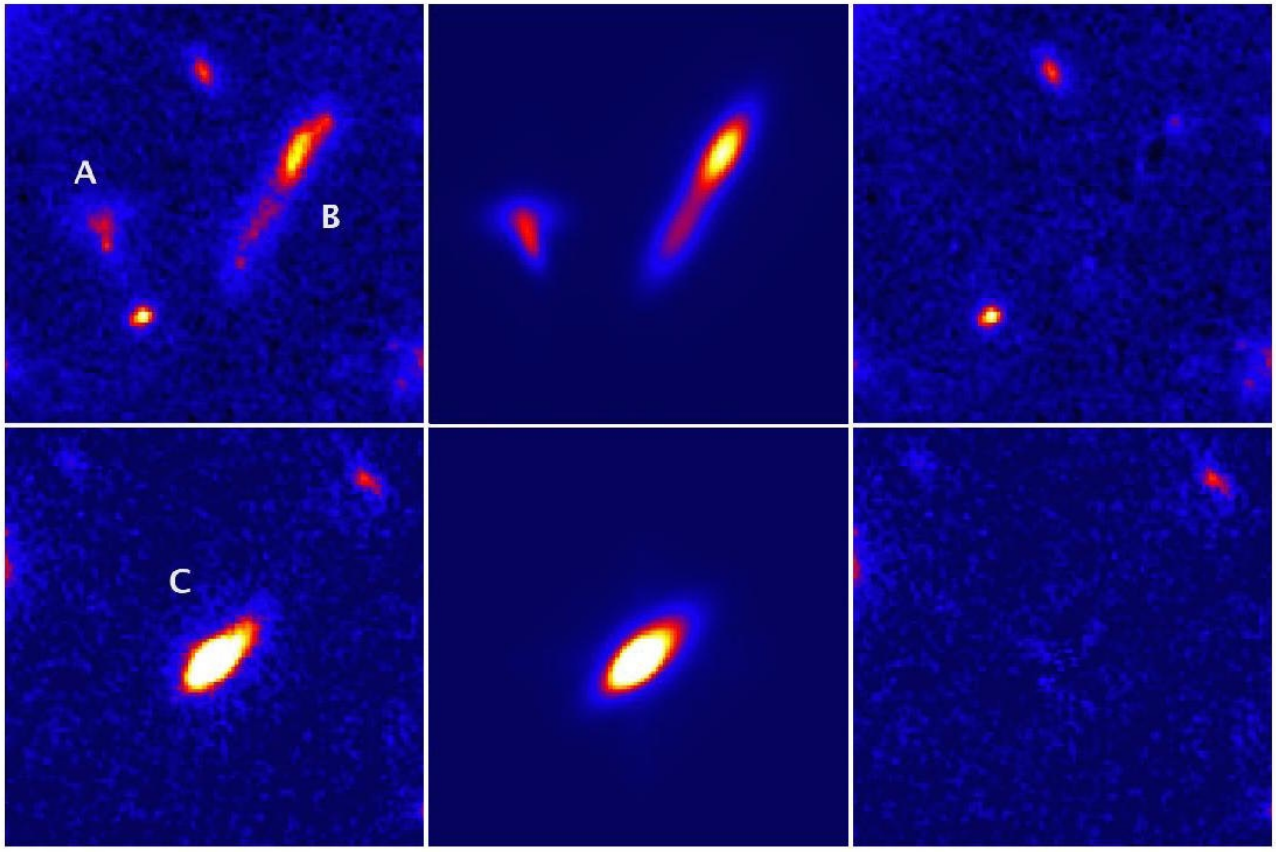

Fig. 2. (Left panel) The HST F160W cutouts of Galaxies-A and B (top) and Galaxy-C (bottom) used for the morphological model fitting. (Middle and right panels) The GALFIT returned models and residuals of the same cutouts. In the latter, only the RO-1001 galaxy models have been subtracted. The rest of the sources, although used during the fit, have been left in the image.

И правда, диски - вращаются

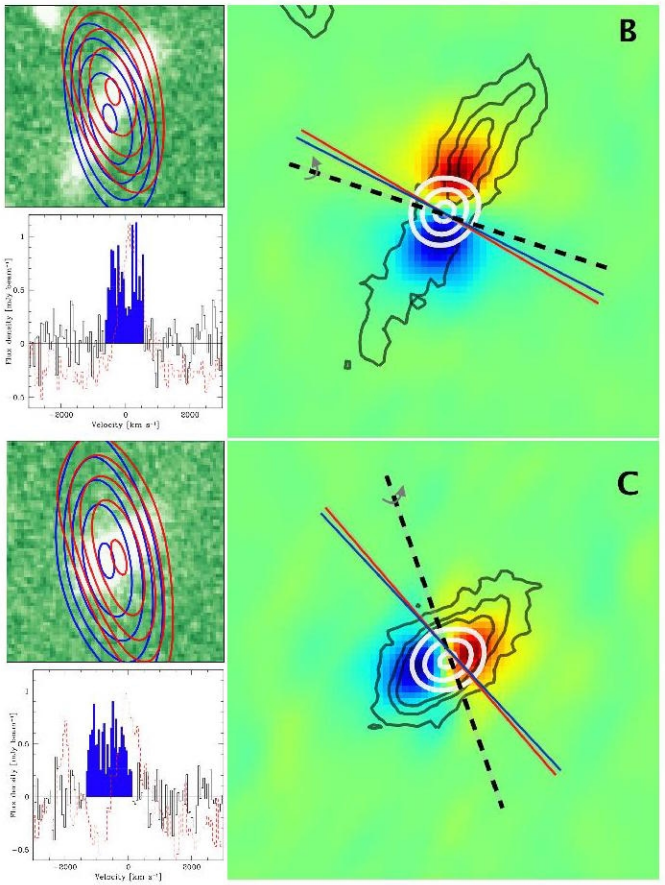

Fig. 7. Two panels showing the rotational properties in Galaxies B and C with three individual sub-images: (top-left) the NOEMA CO[3 – 2] emission profiles for the *blue* and *red*-shifted sections with respect to the average galaxy profile shown as contours superimposed on the F160W image; (bottom-left) The NOEMA spectra with the CO[3 – 2] emission line in blue and the local Lyman-α profile in red; (right) The contours of the stellar disk (black; beginning at 8σ with increments of 4σ), the compact core (white; beginning at 100σ with increments of 50σ for Galaxy-B and at 50σ with increments of 25σ for Galaxy-C) and a representation of the *blue* and *red*-shifted CO[3 – 2] emission locations with the size of the compact core as seen in ALMA. The expected rotational axes have been also been provided for each component – disk in red, core in blue and CO[3 – 2] emission as black dashed lines. The NOEMA spin axes uncertainties are large enough to make the difference with the other component not statistically significant.

… но не образуют звезды

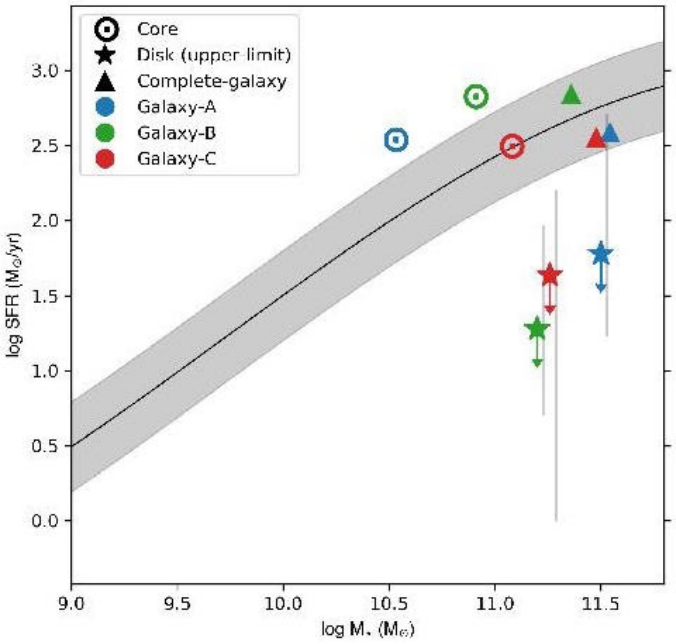

Fig. 3. Components of the three galaxies on the star-forming main-sequence: star-bursting bulges and quiescent disks. The SFR vs stellar-mass values of the star-bursting core, the quiescent stellar disk and the combination of the two placed with respect to the star-forming main-sequence (Schreiber et al. 2015) at z = 3, shown as the black solid line. The shaded region demarcates the 0.3 dex uncertainty in the relation. We use the 3σ ALMA upper-limits as the value for SFR with the associated grey error-bars showing the range allowed by our SED model fitting.The latter have been artificially offset in the x-axis to emphasize the difference in the method of measurement.

Однобокая аккреция?

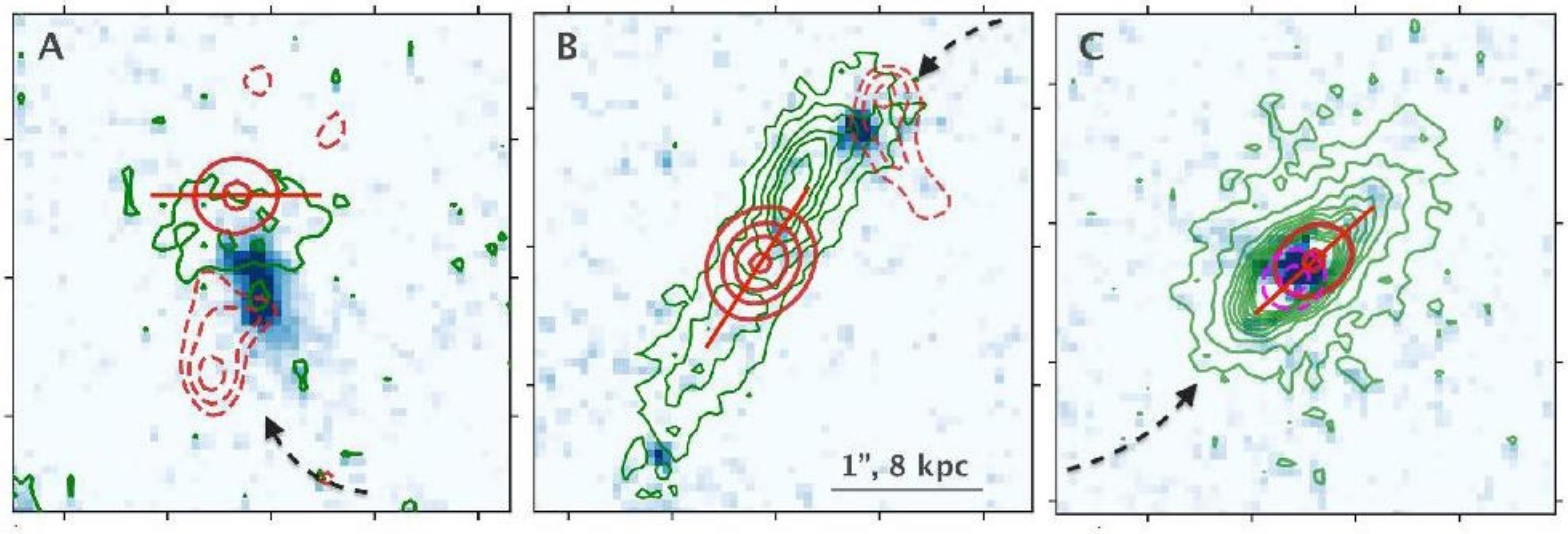

Fig. 9. Additional stellar and dust components tracing the direction of accretion. The three panels showing the three residual F160W images of the galaxies after the subtraction of the primary disks (in green contours; starting at 4σ with increments of 4σ). The red solid contours show the ALMA 870 μm emission with the lines starting at 50σ with increments of 50σ. The red solid lines indicate the respective ALMA major axes. In case of Galaxies A and B, the dashed red contours starting at 3σ with steps of 0.5σ displays the ALMA residual emission after the subtraction of the primary emission regions. In case of Galaxy-C, the same contours show the additional point source adjacent to the core that was found during the fitting procedure. In this case, the contours are at $15, 25\sigma$. Finally, the arrows indicate the likely directions of gas-accretion onto the galaxies based on the asymmetric distribution of all the aforementioned components, which also coincide with the direction in which the disks are lopsided.